Specific transduction and labeling of pancreatic ducts by targeted recombinant viral infusion into mouse pancreatic ducts

Ping Guo[1], Xiangwei Xiao[1], Yousef El-Gohary[1], Angela Criscimanna, Krishna Prasadan, Christopher Rymer, Chiyo Shiota, John Wiersch, Iliana Gaffar, Farzad Esni and George K Gittes

Specific labeling of pancreatic ducts has proven to be quite difficult. Such labeling has been highly sought after because of the power it would confer to studies of pancreatic ductal carcinogenesis, as well as studies of the source of new insulin-producing β-cells. Cre-loxp recombination could, in theory, lineage-tag pancreatic ducts, but results have been conflicting, mainly due to low labeling efficiencies. Here, we achieved a high pancreatic duct labeling efficiency using a recombinant adeno-associated virus (rAAV) with a duct-specific sox9 promoter infused into the mouse common biliary/pancreatic duct. We saw rapid, diffuse duct-specific labeling, with 50 and 89% labeling in the pancreatic tail and head region, respectively. This highly specific labeling of ducts should greatly enhance our ability to study the role of pancreatic ducts in numerous aspects of pancreatic growth, development and function.

The pancreas is formed during early development by the dorsal and ventral bud, each originating from the endodermal lining of the caudal part of the primitive foregut tube after regional specification by the transcription factors Pdx1, followed by PTF1a.[1,2] The ventral pancreatic bud arises from the base of the hepatic diverticulum and contributes to the formation of the head of the pancreas, with the rest of the pancreas arising from the dorsal pancreatic bud.[3] All pancreatic cell types, including endocrine, acinar, and ductal cells derived from a pool of progenitor cells that express the transcription factors Pdx1, PTF1a, and Sox9.[4–6] Postnatally, PTF1a becomes restricted to the acinar cells; pdx1 is expressed in β cells and δ cells, whereas other markers such as Sox9 and HNF1β are restricted to the pancreatic ducts.[6–9]

Identifying suitable alternate sources of β cells from facultative progenitors in the adult pancreas remains a major focus of diabetes research.[10–14] β-cell neogenesis in the adult pancreas has been proposed to arise from several non-β-cell sources, including acinar cells,[15] islet stem cells,[16] islet α-cells,[17]

and most prominently pancreatic ducts.[18,19] Lineage tracing experiments, using the cre-loxp system, have been used to both support[18] or not support[6,8,9,20] β-cell neogenesis from pancreatic ducts. This discrepancy may be in part due to inefficient labeling of duct cells.

Cre expression in transgenic mice can be used for either tissue or cell-specific labeling, with or without a tamoxifen-inducible (cre-ERT2[21]) system to temporally regulate lineage tracing. Cre-ERT2 under the control of a Sox9 promoter potentially allows spatiotemporal control of lineage labeling of pancreatic duct cells (as well as other non-pancreatic cells such as bile duct cells). However, several caveats and limitations exist with tamoxifen-induced labeling. Tamoxifen administration in pregnant mice can induce abortions[22] and a single dose of greater than 4 mg of tamoxifen in adult mice leads to abnormal liver function tests.[9] Furthermore, the cre-ERT2 system may be leaky, resulting in constitutive rather than inducible activation in some cells.[22] Another drawback is the inefficient labeling of cells. When the cre recombinase was driven by the HNF1β promoter (HNF1βcreER mouse) and

Division of Pediatric General and Thoracic Surgery, Children's Hospital of Pittsburgh, University of Pittsburgh Medical Center, One Children Hospital Drive, Pittsburgh, PA, USA
Correspondence: Dr GK Gittes, MD or Dr P Guo, PhD, Benjamin R. Fisher Chair of Pediatric Surgery and Surgeon-in-Chief, Children's Hospital of Pittsburgh, Chief, Division of Pediatric Surgery, University of Pittsburgh, School of Medicine, Children's Hospital of Pittsburgh, One Children's Hospital Drive, 4401 Penn Ave., Pittsburgh, PA 15224, USA.
E-mail: george.gittes@chp.edu or ping.guo@chp.edu
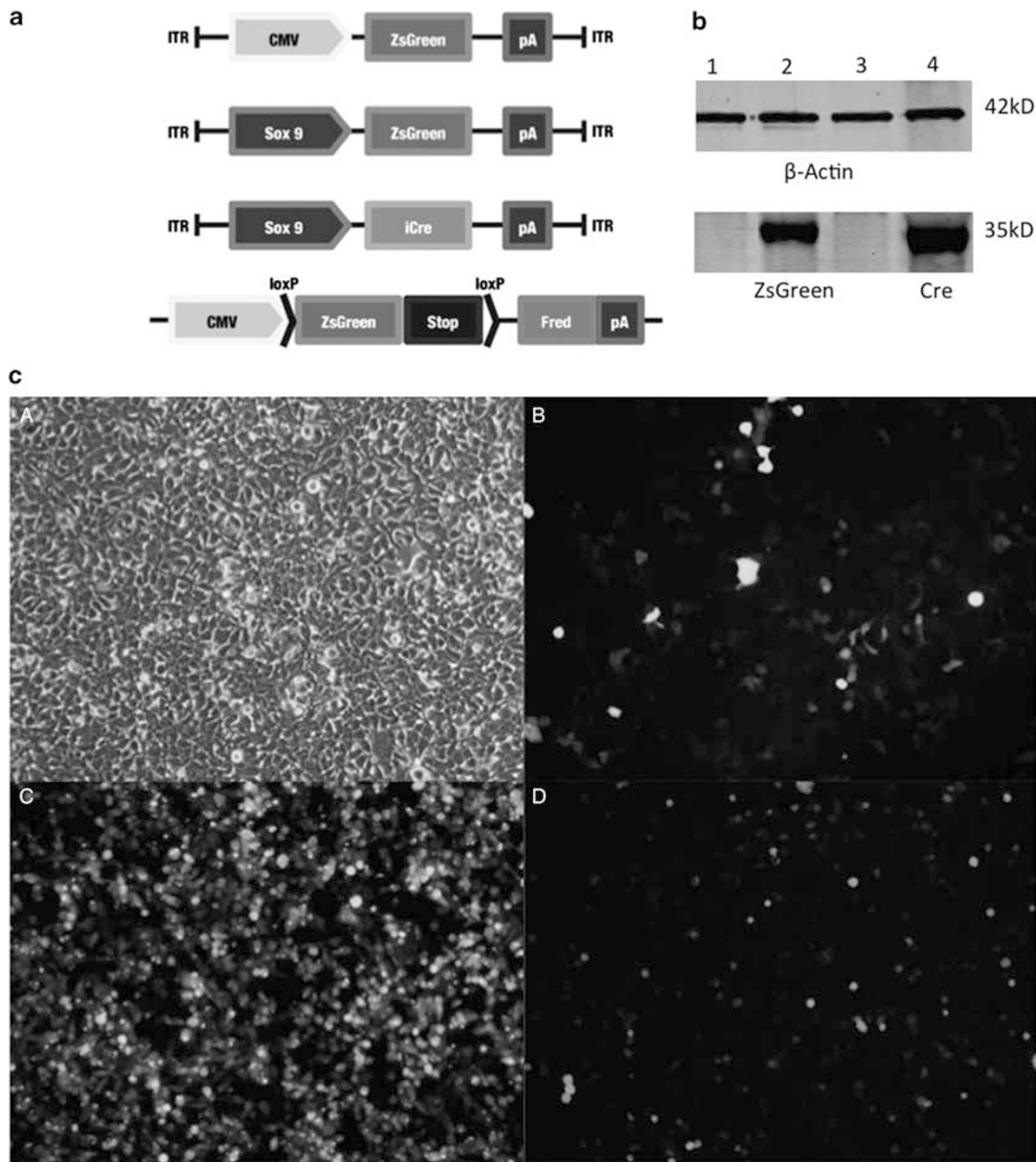[1]These authors contributed equally to the work.

Figure 1 (**a**) Schematic representation of the AAV plasmid constructs used. pAAV-CMV-ZsGreen is a well-established AAV construct.[26,27] The other rAAV plasmid vectors, pAAV-Sox9-ZsGreen, pAAV-Sox9-iCre, and pAAV-CMV-ZsGreen-Stop-Floxed-FarRed were constructed from pAAV-CMV-ZsGreen (see Materials and Methods for details). (**b**) Western Blotting for expression of ZsGreen protein and Cre recombinase from AAV6-Sox9-ZsGreen and AAV6-Sox9-cre virus, respectively. Protein was extracted from HEK293 cells infected with AAV6-Sox9-ZsGreen virus 10 μl of 1.8×10^{12} GCP/ml (lane 2) or 10 ul of 2.3×10^{12} GCP/ml with AAV6-Sox9-cre (lane 4), and non-infection control (lane 1 and 3); 42 kD β-actin was used as control (upper row). (**c**) Determination of GFP and cre expression *in vitro*. The HEK293 cells were infected with AAV6-Sox9-ZsGreen 48hr (bright view in A and green in B); the HEK293/ZsGreen-Lox-Stop-Lox-FarRed cells (C) were infected with AAV6-Sox9-cre 48 h and cre cleavage cells shows red fluorescence (D).

crossed with a Rosa26 reporter mouse to perform lineage tracing of HNF1β promoter activity to analyze a possible ductal contribution to β-cell mass expansion during regeneration, only 1–2% of embryonic and 40% of adult pancreatic duct cells were lineage labeled.[8,23]

To address the inherent problems associated with pancreatic duct labeling, especially the issues of low labeling efficiencies and unpredictable tamoxifen sensitivity, we utilized an adeno-

associated virus (AAV serotype 6), ductal infusion approach.[24] Our goal here was to provide a better tool to more accurately assess for any ductal contribution to newly forming cells in different regeneration models. We first used a Sox9 promoter (468 bp short promoter) to generate a recombinant virus carrying a reporter GFP (AAV6-Sox9-GFP). This recombinant virus construct was then infused into the pancreatic ducts, through the common bile/pancreatic duct, to tag the duct

cells. Sox9 is a transcription factor that has been found to be specifically expressed in the pancreatic ducts.[6,9] After ductal infusion, we only found GFP in pancreatic ducts, not in other pancreatic cells (after 3 days). We also generated a similar AAV vector, but that instead carried a cre recombinase (no ERT) under the same sox9 promoter, and then infused that virus into the common duct of ROSA26flox/Stop/flox-tomato reporter mice (LSL-Tm mice, The Jackson Laboratory strain B6;129S6-Gt(ROSA)26Sor[tm9(CAG-tdTomato)Hze]/J, stock number 007905). One week after injection, it appeared that only the pancreatic duct cells were lineage-tagged and expressed red fluorescence as a result of cre excising the stop cassette. Thus, we report here a very high labeling efficiency and specificity.

MATERIALS AND METHODS
Plasmids and Constructions
Plasmids used in this study include vectors, pAAV-Sox9-ZsGreen (pAAV-Sox9-GFP), pAAV-Sox9-Cre, pAAV-CMV-Cre, and pAAV-CMV-ZsGreen-lox-Stop-lox-FarRed (pAAV-CMV-GFP-Stop-FRed), modified (promoter and gene replacements) from the pAAV-CMV-ZsGreen (pAAV-CMV-GFP) plasmid, which carry the expression cassette flanked by the viral ITRs (provided by Dr. Bing Wang). Far red (Fred) fluorescence protein C–terminus ORF was synthesized by primer extensions.[25] Other plasmids used are a packaging plasmid carrying the serotype 6 rep and cap genes, and a helper plasmid carrying the adenovirus helper functions was purchased from Applied Viromics, LLC. (Fremont, CA). The transgene used in the experiments was ZsGreen (*Zoanthus* sp. green fluorescence protein (GFP) or Cre (Cre recombinase) (under the control of a cytomegalovirus (CMV) promoter or mouse sox9 partial promoter). The AAV-Sox9-GFP construct was designed as shown in Figure 1a. The 5′ and 3′ homology regions (HR) for the Sox9 promoters (1.2 kb –1180 from mouse Sox9 transcript start and 0.5 kb, –468 from mouse Sox9 transcript start, including 21 base-pair of transcript) were amplified by PCR (forward 5′ HR EcoRI-: 5′-GAATT CAAGTGGCCCGTTTTGTCTGGAGTCT-3′, 5′-GAATTCTT CATCGAAAAGTGGGGGTGG-3′, reverse 5′HR NheI-: 5′-GCTAGCGCTCTCGGCTCTCCGACTT-3′, using the C57/ 67 mouse genomic DNA as a template and subcloned into the 5′-EcoRI and 3′-NheI sites of the pAAV-CMV-GFP vector to replace the CMV promoter. For cloning of the pAAV-Sox9-Cre, the ZsGreen was replaced by cre as shown in Figure 1a. The iCre ORF was amplified by PCR (forward 5′ iCre AgeI-: 5′-ACCGGTTGAGCCGCCACCATGGCCAATT TACTG-3′, reverse 5′ iCre NotI-: 5′-GCGGGCCGCTGAGG AGTCCA-3′, using vector pCAG-iCre-GFP as a template. The Sox9 promoters and iCre subclones were confirmed by sequencing.

Cell Culture and AAV-Mediated Gene Expression *In Vitro*
Generation of HEK293-GFP-Stop-FarRed Cells
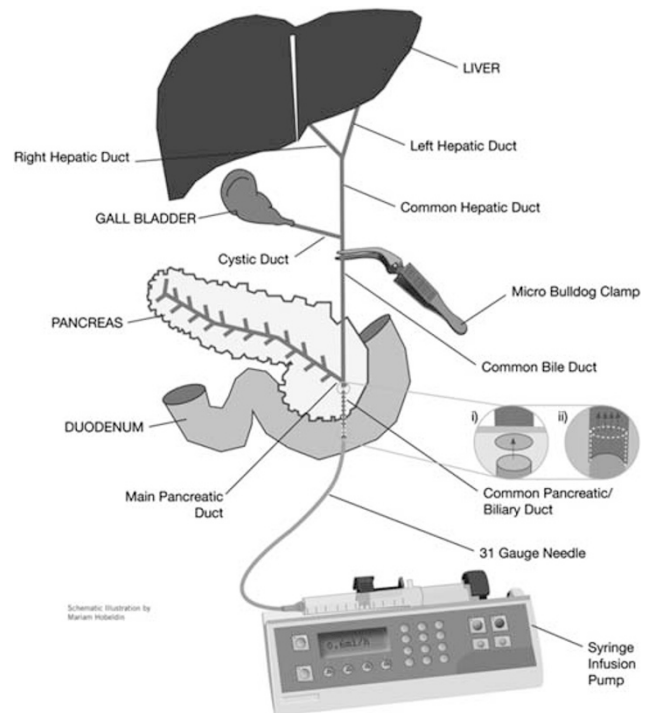The HEK293 cells were cultured in DMEM medium supplemented with 4.0 mM glutamine and 10% horse serum. To

Figure 2 Schematic representation of the viral infusion technique into mouse pancreatic ducts. After the mouse is placed under anesthesia, a midline 1.5 cm laparotomy incision is performed. Duodenum and pancreas along with the pancreatic/biliary ductal system are exposed. A blunt 31gauge needle is connected to a syringe infusion pump, which is set at 0.6 ml/h. A beveled needle is used to make a small puncture wound into the duodenum, to allow the blunted 31gauge needle to be cannulated into the ampulla of Vater, and advanced up to the point just before the branching of the main pancreatic duct (see insets). A micro bulldog clamp is placed on the common bile duct and the infusion is then commenced.

test cre recombination *in vitro*, a stable expression of GFP-stop floxed-FarRed cell line, HEK293/GFP-stop-FarRed, was established. Transfection of pAAV-CMV-GFP-Stop-FarRed plasmid DNA into HEK293 cells was carried out with lipofectamine-2000 reagents in a 12-well culture plate. After reaching 50% confluence, cells were split 1:100 or 1:150 in medium and plated in a 150-mm-diameter cell culture dish. After 2 weeks, single GFP-positive clones were selected under Olympus fluorescence microscope (Olympus SZX12).

Infection of AAV6-Sox9-GFP or cre viruses *in vitro* was performed by adding 10ul of purified virus to a well of 12-well culture plate HEK293 cells or HEK293-GFP-stop floxed-FarRed cells (duplicated wells as well), respectively. After 3 days of infection, the GFP-positive cells from the AAV6-Sox9-GFP-infected wells were visualized under Olympus fluorescence microscope; the red fluorescence cells from the AAV6-Sox9-cre-infected wells were imaged as well under the Olympus fluorescence microscope.

Generation and Purification of AAV Serotype 6 Viruses
Generation and purification of AAV was performed with triple plasmid PEI transfection and PEI/$(NH_4)_2SO_4$ aqueous
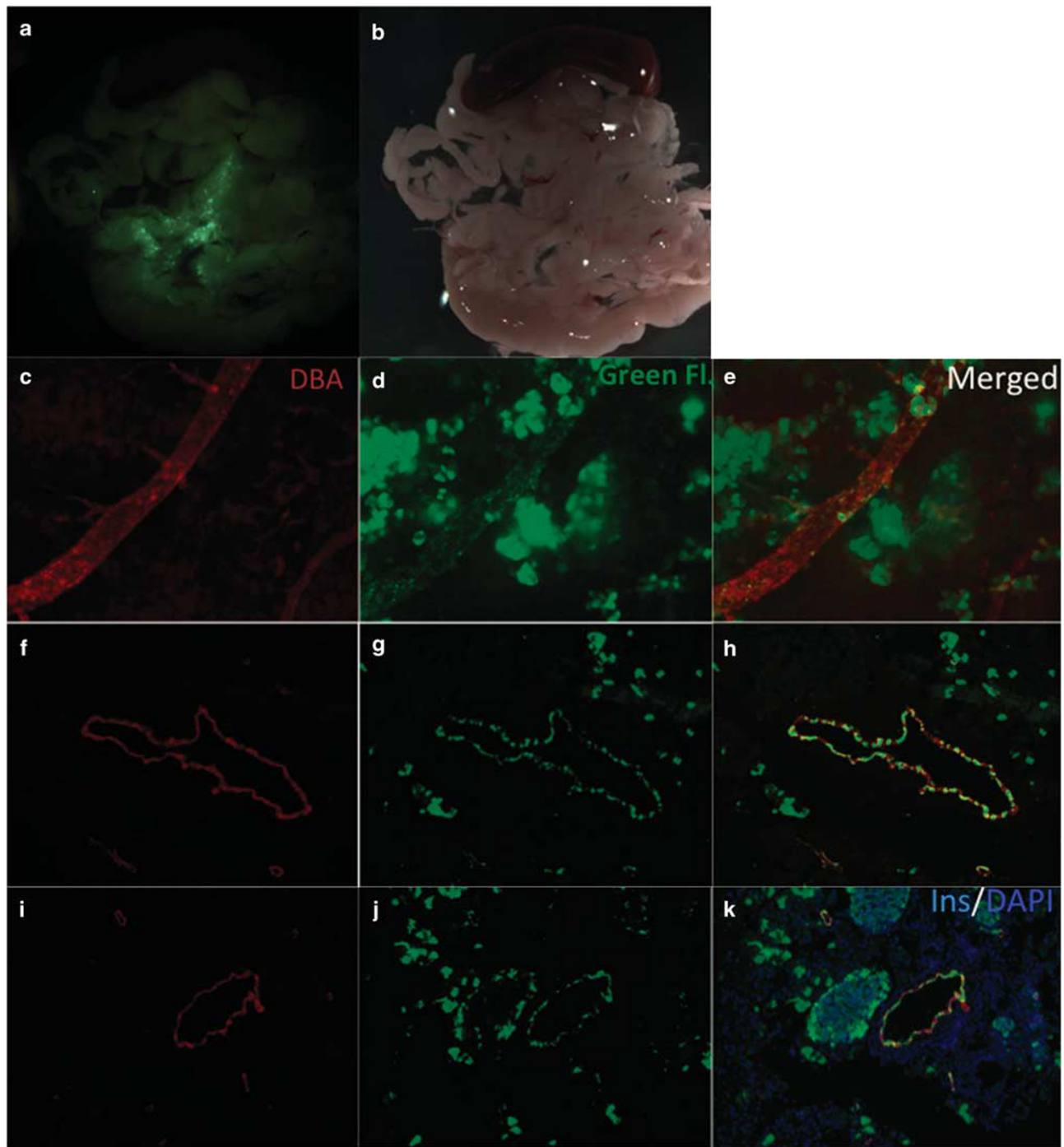
Figure 3 ZsGreen expression in AAV6-CMV-GFP virus-infused pancreatic ducts and islets. The pancreas was harvested 3 days or 1 week after infusion of 100 μl AAV6-CMV-GFP virus, with GFP expression surrounding and in the pancreatic ducts (gross dissecting microscope images at 3 days shown in green in panel **a**, white light image in panel **b**); whole-mount (**c**) and histological section (**f**) of DBA staining for ducts (red in panels **c** and **f**). GFP expression is in and surrounding the pancreatic ducts (**d** and **g**) 1 week after infusion with 100 μl AAV6-CMV-GFP virus. (**e** and **h** are merged images). Immunofluorescence staining for insulin (light blue in panel **k**), DBA (red in panel **l**) and counterstained with DAPI (dark blue in panel **k** merged image) shows that predominantly the periphery of islets are transduced.

two-phase partition.[26,27] Virus titer and AAV-mediated gene transfer assessment was performed as described previously;[26,27] briefly, virus-mediated GFP or cre recombinase gene transfer assay was done *in vitro* in a 12-well culture plate with HEK293 (for AAV6-Sox9-GFP) or HEK293/GFP-stop-Fred cells (for AAV6-Sox9-cre) plated at a density of 0.5×10^6 cells/ml. One microliter of the purified AAV-Sox9-GFP or AAV-Sox9-cre virus was added to each well. At 72 h post
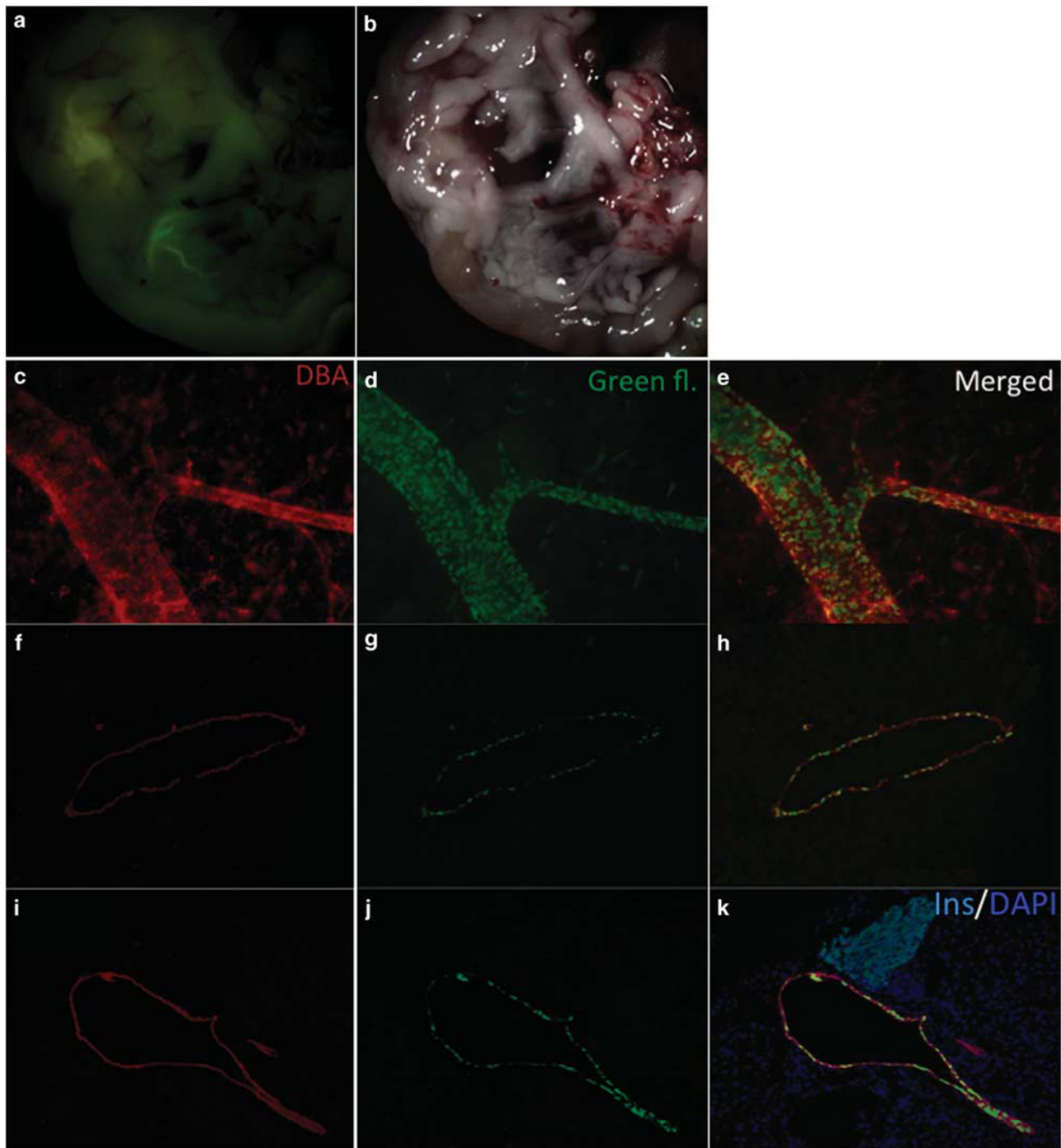
Figure 4 GFP expression specifically in AAV6-Sox9-GFP virus-infected pancreatic ducts. In contrast to AAV6-CMV-GFP infusion, where there was labeling of many non-ductal cells, the pancreas 1 week after infusion with 100 μl AAV6-Sox9-GFP shows GFP expression only in the pancreatic ducts (gross dissecting microscope images shown in panels **a** and **b**). From the whole-mount and histological section staining of DBA (red in panels **c**, and **f**, respectively), GFP expression was seen only in the pancreatic ducts (**d**, **g,** and **j**). Merged images are shown in panels **e, h**, and **k**. Immunofluorescence staining for insulin (light blue in panel **k**), DBA (red in panel **I**) and counterstained with DAPI (dark blue in panel **k** merged images) shows no islet labeling.

infection, GFP fluorescence of cells or Far Red fluorescence of cells were visualized under a Zeiss microscope with 525 nm filter or 700 nm filter. The HEK293 cells were infected with AAV-Sox9-GFP or AAV-Sox9-cre (2.3×10^{12} genome copy particle (GCP)/ml) for 72 h, the cells were harvested at 4 °C and lysed. About 10 ug protein of lysates were separated on a 10%SDS polyacrylamide gel and transferred onto a nitrocellulose membrane. The membrane was blocked and probed
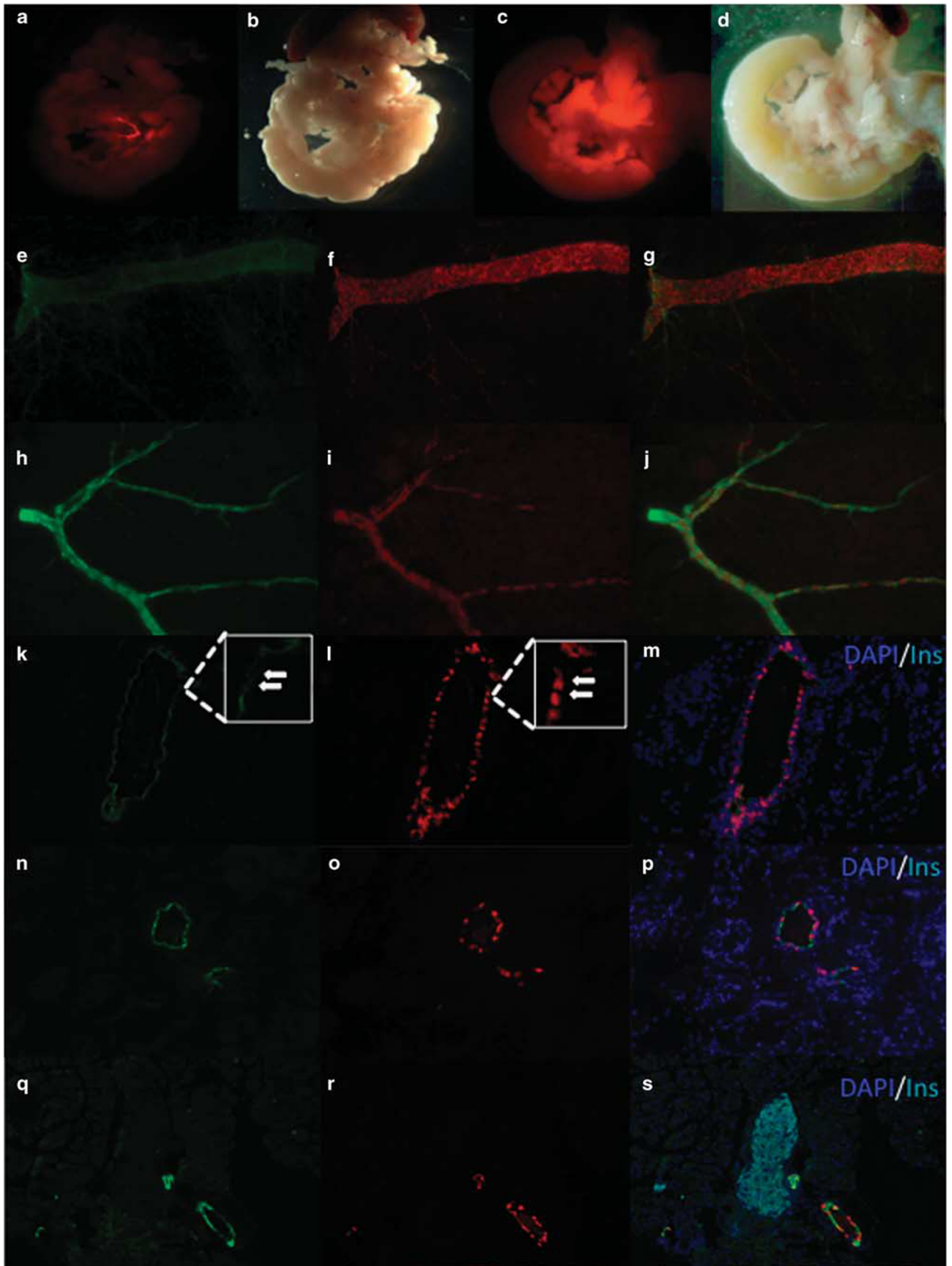
Figure 5 Continued.

with an anti-ZsGreen (Clontech Laboratories, Mountain View, CA) and anti-Cre antibodies (EMD Chemicals, Merck KGaA, Darmstadt, Germany), followed by anti-rabbit-conjugated HRP secondary antibody. ZsGreen and Cre proteins in the blot were visualized by chemiluminescence.

AAV-Mediated Gene Transfection and Pancreatic Ductal-Specific Labeling *In Vivo*

All animal procedures were performed with prior approval of the University of Pittsburgh Institutional Animal Care and Use Committee. Viral gene transfer *in vivo* into adult CD1 mice was performed at 10 weeks of age. For the GFP gene pancreatic ductal transformation, the anesthetized 10-week-old CD1 mice ($n = 8$) were infused with $100\,\mu$l of AAV6-CMV-GFP (titer 2.31×10^{12} GCP/ml) or AAV6-Sox9-GFP (titer 2.35×10^{12} GCP/ml) through the common pancreatic/biliary duct (Figure 2). The infusion was given at a rate of $10\,\mu$l/minute. A clip was placed on the bile duct near the hilum of liver to temporarily occlude the common hepatic duct, leading to specific perfusion of the pancreatic ducts; the ROSA26flox/Stop/flox-tomato reporter mice (LSL-Tm mice) were used for AAV6-Sox9-cre pancreatic ductal transformation and cre recombinase cleavage *in vivo*. The same infusion technique was utilized for the AAV6-Sox9-cre pancreatic ductal tagging assay, the anesthetized 10-week-old LSL-Tm mice ($n = 5$) were infused with $100\,\mu$l of AAV6-Sox9-cre (titer 2.33×10^{12} GCP/ml) through the common pancreatic/biliary duct.

The 10-week-old LSL-Tm mice were injected with AAV6-Sox9-cre through viral infusion, and 4 weeks after viral infusion caerulein (Sigma-Aldrich, catalog number C9026) was injected (50 ug/kg) for 2 days, once every hour for 6 h each day to destroy acinar cells and to study regeneration.[28]

Whole-Mount Staining and Immunohistochemistry

Whole-mount immunofluorescence staining was carried out as described previously.[29–31]

In brief, mice were infused with 10 ml PBS, followed by 10 ml 4% paraformaldehyde (PFA). The pancreatic tissues were then harvested and fixed in 4% PFA for 2 h in 4 °C. Pancreas was then minced into small pieces (0.5 mm × 0.5 mm) and then 100 pieces of pancreas were placed per well (3–4 wells) in a 24-well plate. About $1000\,\mu$l of PBS was added per well, washed on a rotator in PBS for 10 min three times at room temperature (RT) and then washed serially in methanol for 15 min at RT five times. The samples were blocked With 10% normal donkey serum (NDS) in 0.1% PBST for 45 min at RT, incubated with primary antibody in 1% NDS in 0.1% PBST at 4 °C on a rotator overnight, washed with 0.1% PBST on a rotator at RT once an hour for 5 h,
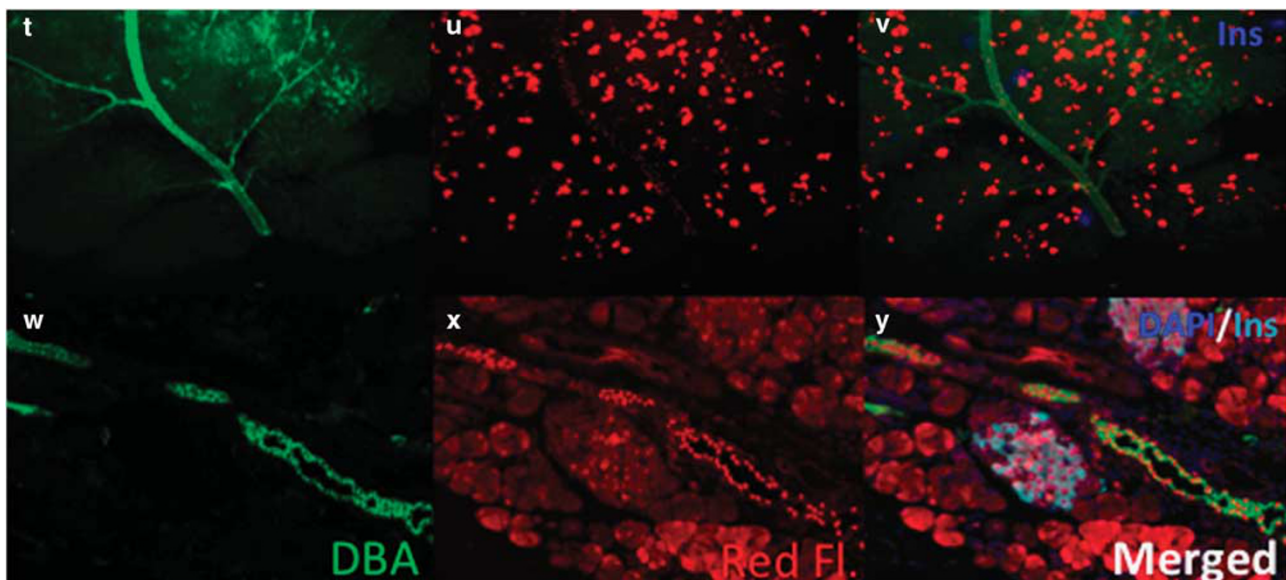

Figure 5 Expression of sox9-cre in the pancreatic ducts of LSL-Tm mice. Cre-induced lineage-tagging (red fluorescence) was seen in the pancreatic ducts of LSL-Tm mouse pancreas 1 week after AAV6-Sox9-cre virus infusion (gross dissecting microscope images shown in panel **a**, fluorescent, and **b**, white light). However, the CMV promoter-driven cre was expressed in many non-ductal cells (gross dissecting microscope images shown in panels **c**, fluorescent, and **d**, white light). Whole-mount staining of DBA (green in panels **e** and **h**), and histological section staining of DBA (green in panels **k**, **n**, and **q**) show Sox9-cre-induced lineage-tagging specifically of LSL-Tm mouse pancreatic ducts (**f**, **i**, **l**, **o** and **r**), including main ducts (**f** and **l**), interlobular and intralobar ducts (**i**, **o** and **r**). The sections are counterstained with DAPI in the merged images (**m**, **p** and **s**). Insets in panels **k** and **l** demonstrate red fluorescent-labeled cells that are DBA-negative stained, but appear to be ductal as they are in the wall of the duct. Whole-mount staining of CMV promoter-driven cre virus-infused pancreas shows Cre recombination also occurred in acinar cells and islets (**t**, **u**, and **v**). In histologic sections, immunofluorescent staining and diffuse Cre-induced red fluorescence in the AAV6-CMV-Cre infused pancreas is shown (**w–y**), insulin (light blue), DBA (green).

incubated with secondary antibody in 1% NDS in PBST at 4 °C on rotator overnight, washed six times with 0.1% PBST on rotator at RT for 10 min, and mounted on chamber slides with whole-mount media and coverslip.

Immunostaining was Performed as described before.[32] Briefly, pancreas was excised and fixed in 4% PFA for 12 h (overnight), 30% sucrose penetrated, embedded in Tissue Tek OCT followed by freezing by immersing into liquid nitrogen. Frozen blocks were stored at -80 °C until sectioning (5 μm). Anti-insulin antibody was purchased from DAKO (DAKO North America, Carpinteria, CA). Cy5-conjugated donkey anti-guinea pig antibody was purchased from Jackson Immunoresearch Laboratories (West Grove, PA).

Quantification and Statistical Analysis

All results are given as the mean ± s.d. One week post injection the pancreata were harvested, sectioned (5 um), and stained with fluorescent lectin Dolichos Biflorus Agglutinin (DBA, a ductal marker) and DAPI. A total of 100 sections were counted for the number of virus-tagged cells (GFP$^+$ or tomato-red$^+$), DBA$^+$ cells (indicating the number of duct cells as a denominator), and DAPI$^+$ cells to confirm that the DBA$^-$ cells that were GFP$^+$ or tomato-red$^+$ were, in fact, cells. The average number of GFP$^+$ and DBA$^+$ (rhodamine conjugated) cells were calculated for the AAV6-Sox9-GFP-transduced pancreas. To document viral-induced cre-linage tagging, tomato-red$^+$ and DBA$^+$ (FITC-conjugated) cells were counted in the AAV6-Sox9-cre-transduced pancreas. A total of 3000 acini or 1000 islet and 1000 ductal cells from each pancreas were counted for cre-recombinant red fluorescent lineage-tagged cells after caerulein treatment and compared with control pancreas (saline or non-caerulein treatment). GFP or red fluorescence-positive cells were compared using Student's t-test. Differences were considered statistically significant when the P-value was <0.05.

RESULTS

Pancreatic Endocrine and Exocrine Cells are Efficiently Transduced After Intraductal Infusion of AAV6-CMV-GFP

AAV serotype 6 has been reported to have tropism for the mouse pancreas and pancreatic ducts in particular.[24] Therefore, we infused 100 μl of 2.35×10^{12} GCP/ml of AAV serotype 6 vector encoding ZsGreen (GFP) driven by the CMV promoter into the pancreas via cannulation of the common pancreatic/biliary duct in 10-week-old CD1 mice (Figure 2). At 3 days post infusion, expression of GFP throughout the pancreas and pancreatic ducts was seen (Figures 3a and b). At 1 week after the infusion, islets expressed GFP, especially at the periphery, as did acinar cells (Figure 3). Pancreatic ducts appeared to be transduced with high efficiency (Figure 3). Double immunostaining for insulin and DBA confirmed that pancreatic ducts and islets were transduced (Figure 3). There was no obvious decline in GFP signal 4 weeks after intraductal administration of AAV6-CMV-GFP (data not shown). Our results confirm that

AAV6 is suitable for long-term (at least 4 weeks) transduction of pancreatic cells using an intraductal viral infusion technique.

Pancreatic Intraductal Delivery of AAV6-Sox9-GFP Leads to Duct-Specific Expression

We next combined the relatively selective AAV serotype 6 ductal tropism together with a duct-specific promoter, a sox9 promoter, to drive gene expression only in pancreatic ducts. The mouse sox9 promoter was assembled into the AAV vector, replacing the CMV promoter (Figure 1a). Sox9 is expressed in human embryonic kidney cells,[33] thus HEK293 cells were infected with AAV-Sox9-GFP using two different sizes of sox9 promoters (468 bp and 1125 bp). Both were found to have similar transduction in the HEK293 cells 3 days after infection, but the 1125 bp promoter appeared to display stronger expression. However, we then tested the effectiveness of the sox9-cre in HEK293 cells harboring a GFP-stop floxed-Fred (Far Red) construct. The 468 bp sox9 promoter was chosen for *in vivo* experiments as it was adequate to drive cre expression and cre-induced recombination. The AAV6-Sox9-GFP virus was infused into pancreatic ducts as described in the methods. At 3 days, 1 week, and 4 weeks post infusion (with 100 μl of 2.35×10^{12} GCP/ml virus), the transduction specificity and efficiency of GFP in pancreatic ducts were examined. Under the dissection microscope, GFP fluorescence was only seen in pancreatic ducts (Figure 4). Whole-mount staining for DBA and GFP revealed efficient and specific transduction of pancreatic ductal cells (Figures 4c–e). Immunostaining of tissue sections confirmed the specificity of AAV6-Sox9-GFP transduction of pancreatic ductal cells (Figures 4f–h), with no islet nor acinar cell labeling seen (Figures 4i–k). No apparent loss of GFP expression was seen at 4 weeks (Supplementary Figure 1).

Intraductal Delivery of AAV6-Sox9-Cre Leads to Recombination and Lineage-Tagging only in Pancreatic Ductal Cells

The *Cre-loxp* recombination is widely used to achieve gene deletions, insertions, and translocations in the DNA of cells. To examine whether AAV serotype 6 with a Sox9 shorter promoter driving cre recombinase would only tag pancreatic ducts, improved cre (iCre) was assembled into the above AAV-Sox9-GFP vector with replacement of the GFP (Figure 1a), and then 100 μl of 2.34×10^{12} GCP/ml AAV6-Sox9-cre virus was infused into the pancreatic duct of 10-week-old adult LSL-Tm reporter mice, which express tomato-red in all cre-recombined cells and their progeny. AAV6-CMV-cre virus was infused into the pancreatic duct of 10-week-old LSL-Tm reporter mice as a control. Pancreata were harvested at 3 days, 1 week, and 4 weeks after intraductal infusion. Under a dissection microscope, it appeared that tomato-red fluorescence was only present in the pancreatic ducts (Figures 5a and b). The AAV6-CMV-Cre viral-infused pancreas had red fluorescence throughout the pancreas (Figures 5c and d). Whole-mount staining demonstrated
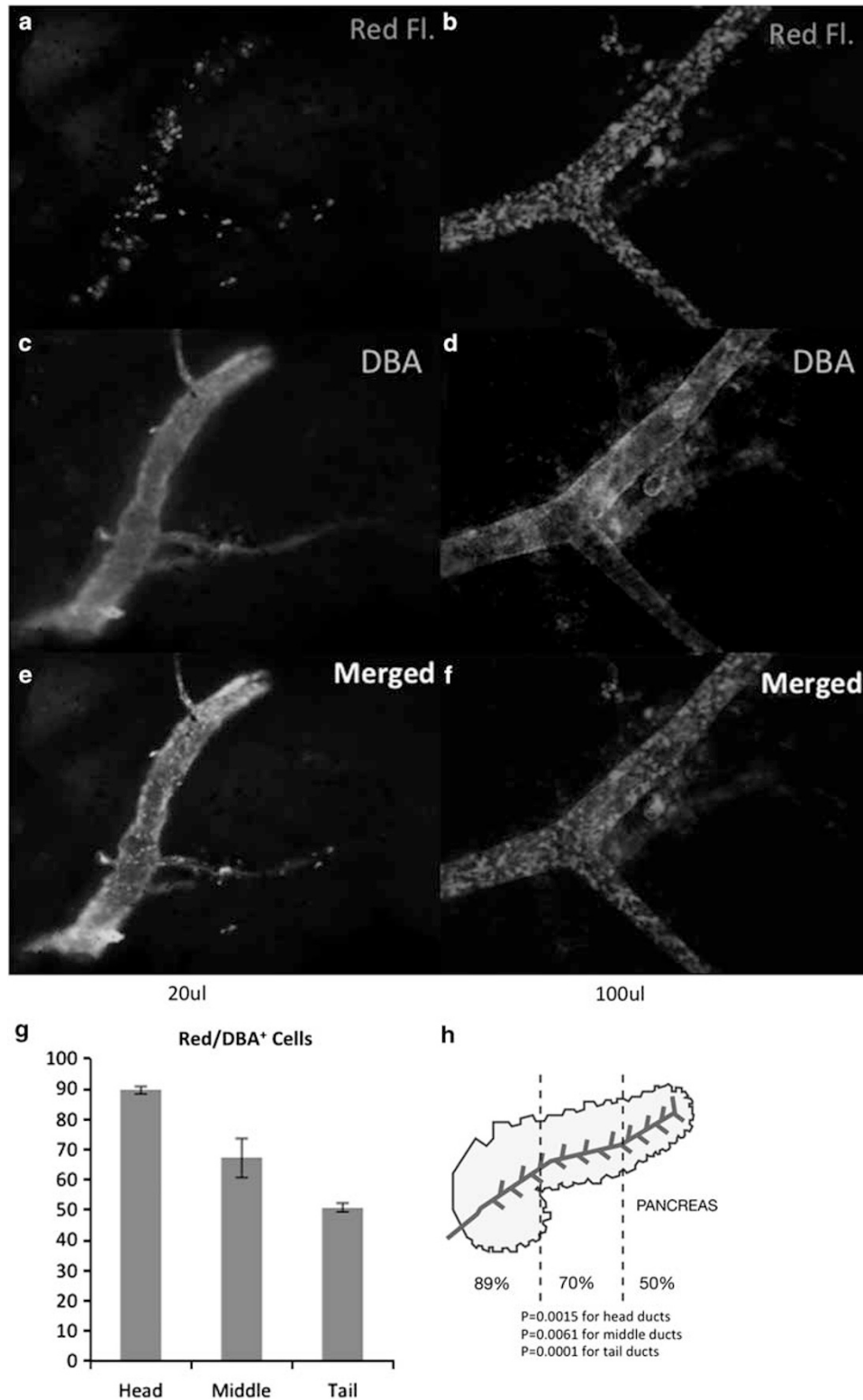
Figure 6 Dose-dependent cre-tagging of pancreatic ducts and quantification of cre efficiency. Cre-tagging (red in panels **a** and **b**) increases with the volume of virus infusate in LSL-Tm pancreatic ducts. DBA (green in panels **c** and **d**) and merged images (**e** and **f**) showing the density of Cre-tagged cells in the infused pancreatic ducts with 20 μl (**a**, **c**, and **e**) and 100 μl (**b**, **d** and **f**) of AAV6-Sox9-Cre virus, respectively. Quantification of cre-tagging efficiency in the pancreatic ductal tree after infusion of 100 μl of AAV6-Sox9-Cre virus (**g**). The pancreas schematic figure (**h**) represents the percentage of cre-tagged ductal cells in the head, middle, and tail of the pancreas after a 100-ul infusion.

strong red fluorescent co-staining with DBA in the main pancreatic ducts (Figures 5e–g), indicating that the main pancreatic ducts were efficiently labeled by cre. The interlobular and intralobular ducts also showed efficient labeling (Figures 5h–j). By histologic sections tomato-red was seen in pancreatic ductal cells, both in the main ducts (Figures 5k–m) as well as in smaller branches (Figures 5n–s). Some labeled cells appeared to be in the wall of the DBA$^+$ ducts, but were themselves DBA$^-$ (Figures 5k and l) (see quantification below), but red fluorescence was observed in <0.1% of islet cells and acinar cells (Figures 5m, p, and s). In the AAV6-CMV-cre virus-infused pancreata, red fluorescence was seen throughout the pancreas (Figures 5t, u, and v in whole-mount and Figures 5w, x, and y in histologic sections).

To determine whether virus load and/or volume of infusate affects sox9-cre activity in the pancreatic ducts, we infused different volumes of AAV6-Sox9-cre virus at a constant viral particle titer of 2.34×10^{12} GCP/ml into the LSL-Tm mice. At 20 ul of infusate, cre-tagged cells were observed in the main ducts and interlobular branches, but at a lower efficiency (Figure 6a). When 100 μl was infused, there was an appreciable increase in pancreatic ductal labeling efficiency as evident on whole-mount images (compare Figures 6 a, b–e, and f). With this 100 μl volume infusion, we saw extensive labeling of the pancreatic ducts in the pancreatic head, middle, and tail (see later section for quantification).

The volume of the mouse pancreatic ductal tree would presumably depend on the size of the mouse, but the maximum volume infused into a 30-g LSL-Tm mouse was 145 μl, which still led to high efficiency and specific cre recombination of only pancreatic duct cells (data not shown), though presumably with an increased risk of pancreatitis.

Quantification of Cre-Tagged Cells After Sox9-Cre Viral Infusion into LSL-Tm Mice Pancreatic Ducts

Three LSL-Tm mouse pancreata, 1 week after AAV6-Sox9-cre viral infusion with 100 μl of 2.34×10^{12} GCP/ml, were stained for the ductal marker DBA and DAPI for nuclei. A total of 20 sections from each pancreas were chosen for quantification analysis of cre recombinase efficiency. The red fluorescent ductal cells, DBA-positive cells and DAPI-stained ductal cells from the pancreatic head, middle, and tail were counted under a Zeiss microscope at $\times 200$ magnification. The colocalized DBA-positive and DAPI-stained nuclei were defined as pancreatic ductal cells. Red fluorescence located in a DAPI/DBA-positive cell was counted as a cre-tagged pancreatic ductal cell. In the pancreatic head, the cre-tagging was highly efficient, with 89% of DAPI/DBA-positive pancreatic ductal-labeled cells; in the mid-portion and tail of the pancreas, red cells were 70% and 50%, respectively (Figures 6g and h). With AAV-Sox9-cre viral infusion, only 5% of DBA$^-$ or DBA-weak cells had red fluorescence (Figures 5k–i and Supplementary Figure 1). These labeled DBA-negative or DBA-weak cells appeared to be exclusively localized to the duct wall, and therefore likely represent DBA$^-$ duct cells as

shown in representative images (Figures 5k, l, m, and p). On the other hand, the AAV6-CMV-cre recombinant viral-infused pancreas in the LSL-Tm mice had up to 55.5839% ± 0.027926 DBA$^-$ or DBA-weak cells labeled with red fluorescence (Figures 5t–y and Supplementary Figure 1), most of which were localized outside the duct wall.

Labeling of Regenerating Pancreatic Cells with Pancreatic Ductal Viral Infusion of AAV6-Sox9-cre Virus

To determine if our AAV6-Sox9-Cre viral pancreatic ductal infusion is a viable approach for duct lineage-tagging, we first administered caerulein to the LSL-Tm mice 4 weeks after viral infusion. The mice were treated with caerulein for 2 days, as described in the methods. The caerulein-treated pancreata were harvested after 3 days, 1 week and 3 weeks. Caerulein treatment induced pancreatitis with typical cytoplasmic vacuolization structures seen 3 days after caerulein treatment (Figure 7b). Three weeks after caerulein treatment, the normal morphology of acinar cells was regenerated (Figure 7c). Acinar-to-ductal metaplasia was seen by DBA staining at 3 days after caerulein treatment, but cre-recombinant red fluorescent cells were still seen only in the main pancreatic ducts (89.0% in the pancreatic head), not the metaplastic ducts (Figures 7g–i). Similarly, 99.9% of the new regenerated acinar cells were not labeled with cre-targeted red fluorescence (Figures 7j–l). Less than 0.1% of acinar cells were red fluorescent after caerulein treatment (Figure 7m) (see methods for quantification technique). These results suggest that regenerated acinar cells in caerulein-treated pancreas do not derive from cre-labeled-pancreatic ducts.

DISCUSSION

The Cre/LoxP system has proven to be a useful tool in many model systems.[6,9,18,22] It allows for spatial and temporal control of gene expression, but in many systems the utility of cre-loxP is dependent on the properties of the promoter and its expression pattern. Furthermore, cre-loxP-mediated DNA recombination allows for gene function analyses and lineage-tagging, both during embryonic development and in mature mice. However, off-target effects and poor temporal regulation have limited the applicability of cre-loxP in many experimental systems, especially when using a tamoxifen-inducible system.[9,22,8,23]

AAV-mediated cre recombinase expression is a relatively simple and efficient method for lineage-tagging and altering gene expression *in vivo*.[34,35] However, one drawback with its use in the pancreas is inadequate labeling of pancreatic cells, especially pancreatic ductal cells.[24] Here we report that the combination of AAV serotype tissue tropism, with a specific gene promoter, together with ductal infusion of virus, leads to successful *in vivo* labeling of pancreatic ducts. After examining the entire pancreas of 15 wild-type CD1 mice infused with AAV6-Sox9-GFP, and 9 LSL-Tm reporter mice
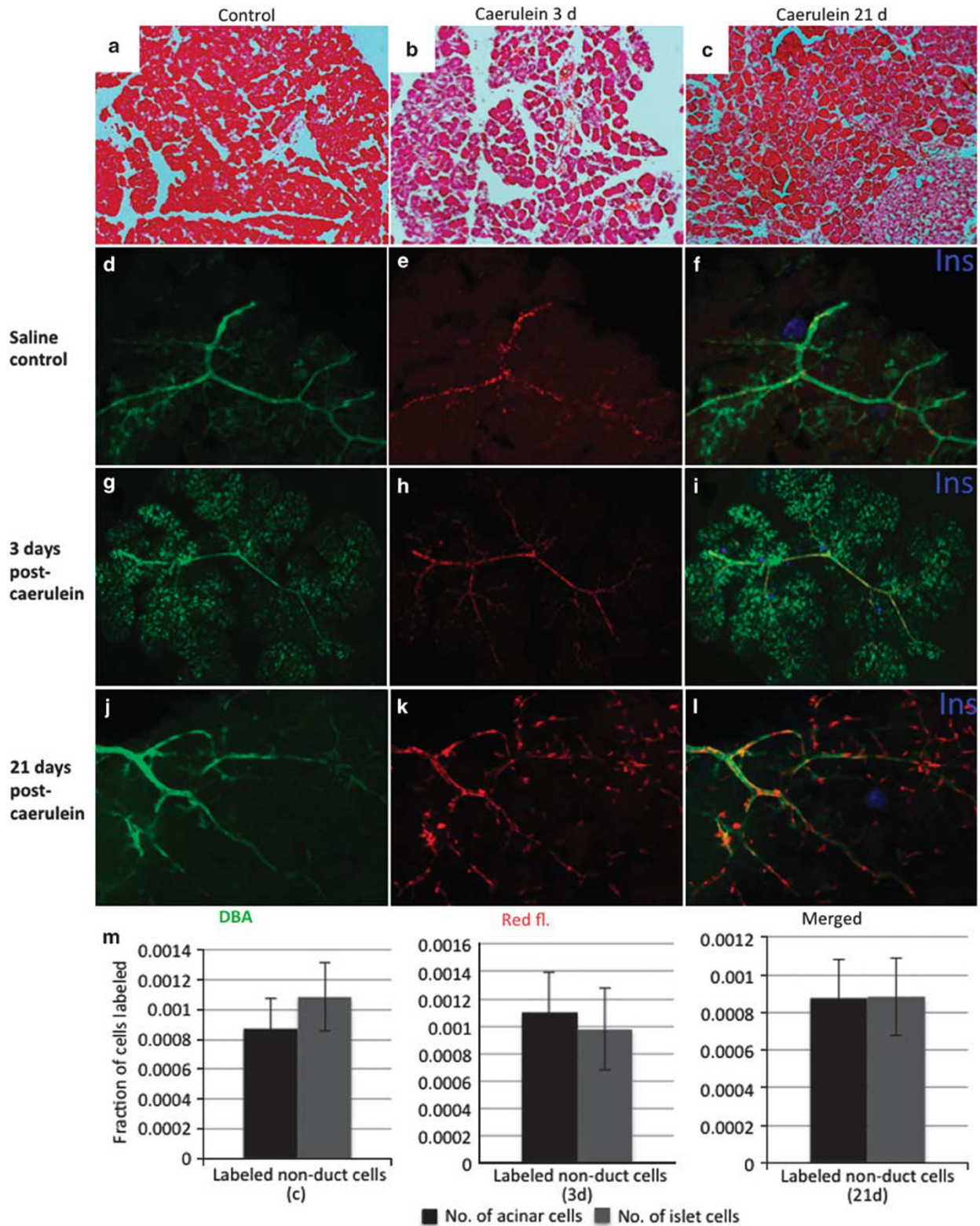
Figure 7 Lineage-tagging of ducts during acinar regeneration after caerulain treatment. LSL-Tm mice were infused with AAV6-Sox9-Cre virus into the pancreatic ducts at 10 weeks of age. Four weeks after viral infusion, mice were treated with either caerulein or saline injections for 2 days and analyzed 3 days, 1 week, and 21 days later. H&E staining shows cytoplasmic vacuolization at 3 days after caerulein treatment (**b**); saline-injected group at 3 days is normal (**a**). Twenty-one days after caerulein treatment, the pancreas shows recovery of normal histology (**c**). Whole-mount staining reveals that the main pancreatic ducts were tagged with red fluorescence at 4 weeks after AAV6-Sox9-Cre viral infusion (**d–f**). Three days after caerulein treatment, the acinar-to-ductal metaplastic tubules were stained with DBA, but the recombinant red fluorescence was only seen in the pancreatic main ducts (**g–i**). Twenty-one days after caerulein administration the recombinant red fluorescent pancreatic ducts still persisted, but no red acini were seen (**g–i**).

receiving AAV6-Sox9-cre virus, we found <0.1% labeled non-ductal cells.

AAV6 virus with CMV promoter appears to infect most cells in the pancreas (Figures 3d, e, j, k; Figures 5u, v, x, y). In the adult mouse pancreas, the sox9 promoter is most active in the pancreatic ducts.[6,9] In other pancreatic cells, however, such as acinar cells and endocrine cells, sox9 promoter activity is low,[9,36] unlike the CMV promoter, which has strong activity in acinar and islet cells (Figures 3d, e, j and k; Figures 5t–y). Hence, by using a short sox9 promoter, together with the serotype tissue tropism of AAV6, we achieved cre recombinase activity specially in pancreatic ducts. We believe that this approach now represents the most specific and efficient labeling system available for driving pancreatic duct-specific gene expression or for duct lineage-tagging.

Caerulein injections induce pancreatitis through dysregulation of digestive enzyme production and cytoplasmic vacuolization, leading to acinar cell death and pancreatic edema. In caerulein-induced pancreatitis, acinar-to-ductal transient metaplasia (ADM) occurs, followed by regeneration or reversion to normal acini.[28,37] To test the possibility that ductal cells contribute to acinar cell regeneration following caerulein treatment, we lineage-tagged the duct cells with AAV-Sox9-cre viral infusion and performed caerulain treatment. Acinar-to-ductal metaplasia was observed 3 days after caerulein treatment (Figures 7g–i). Though these metaplastic tubules were stained with DBA, they were not tomato-red. Three weeks post caerulein treatment, the regenerated acinar cells also did not label with tomato-red, suggesting that they were not derived from the AAV6-Sox9-cre labeled ducts in LSL-Tm mice (Figures 7j–l and m).

Previous cre-based pancreatic ductal cell lineage tracing experiments have used carbonic anhydraseII-CreERT, CK19-CreERT, HNF1β-CreERT, and Sox9-CreERT mice, but with variable results.[6,8,9,18,20] For over a decade, controversy has existed regarding the source of new insulin-producing β cells in the adult pancreas, especially the possibility that ducts may be such a source. Our ductal labeling method could provide an improved approach, with minimal leakiness and no tamoxifen dependency. This approach, especially in combination with whole-mount imaging, provides an excellent appreciation of pancreatic ductal anatomy and labeling efficiency in the mouse pancreas.[30,31]

In conclusion, AAV6-mediated tissue tropism, combined with a sox9 shorter promoter and direct intraductal viral delivery can achieve durable and specific pancreatic duct tagging. This method, along with whole-mount imaging, should complement existing methods for the study of pancreatic duct lineages.

DISCLOSURE/CONFLICT OF INTEREST
The authors declare no conflict of interest.

1. Grapin-Botton A. Antero-posterior patterning of the vertebrate digestive tract: 40 years after Nicole Le Douarin's PhD thesis. Int J Dev Biol 2005;49:335–347.
2. Moore-Scott BA, Opoka R, Lin SC, et al. Identification of molecular markers that are expressed in discrete anterior-posterior domains of the endoderm from the gastrula stage to mid-gestation. Dev Dyn 2007;236:1997–2003.
3. Gittes GK. Developmental biology of the pancreas: a comprehensive review. Dev Biol 2009;326:4–35.
4. Gu G, Dubauskaite J, Melton DA. Direct evidence for the pancreatic lineage: NGN3 + cells are islet progenitors and are distinct from duct progenitors. Development 2002;129:2447–2457.
5. Kawaguchi Y, Cooper B, Gannon M, et al. The role of the transcriptional regulator Ptf1a in converting intestinal to pancreatic progenitors. Nat Genet 2002;32:128–134.
6. Kopp JL, Dubois CL, Schaffer AE, et al. Sox9 + ductal cells are multipotent progenitors throughout development but do not produce new endocrine cells in the normal or injured adult pancreas. Development 2011;138:653–665.
7. Masui T, Swift GH, Hale MA, et al. Transcriptional autoregulation controls pancreatic Ptf1a expression during development and adulthood. Mol Cell Biol 2008;28:5458–5468.
8. Solar M, Cardalda C, Houbracken I, et al. Pancreatic exocrine duct cells give rise to insulin-producing beta cells during embryogenesis but not after birth. Dev Cell 2009;17:849–860.
9. Furuyama K, Kawaguchi Y, Akiyama H, et al. Continuous cell supply from a Sox9-expressing progenitor zone in adult liver, exocrine pancreas and intestine. Nat Genet 2011;43:34–41.
10. Vennerstrom JL, Arbe-Barnes S, Brun R, et al. Identification of an antimalarial synthetic trioxolane drug development candidate. Nature 2004;430:900–904.
11. Georgia S, Bhushan A. Beta cell replication is the primary mechanism for maintaining postnatal beta cell mass. J Clin Invest 2004;114:963–968.
12. Teta M, Rankin MM, Long SY, et al. Growth and regeneration of adult beta cells does not involve specialized progenitors. Dev Cell 2007;12:817–826.
13. Xiao X, Wiersch J, El-Gohary Y, et al. TGFbeta receptor signaling is essential for inflammation-induced but not beta-cell workload-induced beta-cell proliferation. Diabetes 2013;62:1217–1226.
14. Dor Y, Brown J, Martinez OI, et al. Adult pancreatic beta-cells are formed by self-duplication rather than stem-cell differentiation. Nature 2004;429:41–46.
15. Minami K, Okuno M, Miyawaki K, et al. Lineage tracing and characterization of insulin-secreting cells generated from adult pancreatic acinar cells. Proc Natl Acad Sci USA. 2005;102:15116–15121.
16. Zulewski H, Abraham EJ, Gerlach MJ, et al. Multipotential nestin-positive stem cells isolated from adult pancreatic islets differentiate ex vivo into pancreatic endocrine, exocrine, and hepatic phenotypes. Diabetes 2001;50:521–533.
17. Thorel F, Nepote V, Avril I, et al. Conversion of adult pancreatic alpha-cells to beta-cells after extreme beta-cell loss. Nature 2010;464:1149–1154.
18. Inada A, Nienaber C, Katsuta H, et al. Carbonic anhydrase II-positive pancreatic cells are progenitors for both endocrine and exocrine pancreas after birth. Proc Natl Acad Sci U S A. 2008;105:19915–19919.
19. Wang RN, Kloppel G, Bouwens L. Duct- to islet-cell differentiation and islet growth in the pancreas of duct-ligated adult rats. Diabetologia 1995;38:1405–1411.

20. Kopinke D, Murtaugh LC. Exocrine-to-endocrine differentiation is detectable only prior to birth in the uninjured mouse pancreas BMC Dev Biol 2010;10:38.

21. Indra AK, Warot X, Brocard J, et al. Temporally-controlled site-specific mutagenesis in the basal layer of the epidermis: comparison of the recombinase activity of the tamoxifen-inducible Cre-ER(T) and Cre-ER(T2) recombinases. Nucleic Acids Res 1999;27:4324–4327.

22. Jaisser F. Inducible gene expression and gene modification in transgenic mice. J Am Soc Nephrol 2000;11(Suppl 16):S95–S100.

23. Kushner JA, Weir GC, Bonner-Weir S. Ductal origin hypothesis of pancreatic regeneration under attack. Cell Metab 2010;11:2–3.

24. Jimenez V, Ayuso E, Mallol C, et al. In vivo genetic engineering of murine pancreatic beta cells mediated by single-stranded adeno-associated viral vectors of serotypes 6, 8 and 9. Diabetologia 2011; 54:1075–1086.

25. Gou D, Zhang H, Baviskar PS, et al. Primer extension-based method for the generation of a siRNA/miRNA expression vector. Physiol Genomics 2007;31:554–562.

26. Guo P, El-Gohary Y, Prasadan K, et al. Rapid and simplified purification of recombinant adeno-associated virus. J Virol Methods 2012;183:139–146.

27. Guo P, Xiao X, El-Gohary Y, et al. A simplified purification method for AAV variant by Polyethylene Glycol aqueous two-phase partitioning. Bioengineered 2012;4:2.

28. Kopp JL, von Figura G, Mayes E, et al. Identification of Sox9-dependent acinar-to-ductal reprogramming as the principal mechanism for initiation of pancreatic ductal adenocarcinoma. Cancer Cell 2012;22: 737–750.

29. El-Gohary Y, Sims-Lucas S, Lath N, et al. Three-dimensional analysis of the islet vasculature. Anat Rec (Hoboken) 2012;295:1473–1481.

30. El-Gohary Y, Tulachan S, Branca M, et al. Whole-mount imaging demonstrates hypervascularity of the pancreatic ducts and other pancreatic structures. Anat Rec (Hoboken) 2012;295:465–473.

31. Xiao X, Guo P, Chen Z, et al. Hypoglycemia reduces vascular endothelial growth factor A production by pancreatic beta cells as a regulator of beta cell mass. J Biol Chem, 288:8636–8646.

32. Reginensi A, Clarkson M, Neirijnck Y, et al. SOX9 controls epithelial branching by activating RET effector genes during kidney development. Hum Mol Genet 2011;20:1143–1153.

33. Ahmed BY, Chakravarthy S, Eggers R, et al. Efficient delivery of Cre-recombinase to neurons in vivo and stable transduction of neurons using adeno-associated and lentiviral vectors. BMC Neurosci 2004; 5:4.

34. Kaspar BK, Vissel B, Bengoechea T, et al. Adeno-associated virus effectively mediates conditional gene modification in the brain. Proc Natl Acad Sci USA. 2002;99:2320–2325.

35. Seymour PA, Freude KK, Tran MN, et al. SOX9 is required for maintenance of the pancreatic progenitor cell pool. Proc Natl Acad Sci USA. 2007;104:1865–1870.

36. Jensen JN, Cameron E, Garay MV, et al. Recapitulation of elements of embryonic development in adult mouse pancreatic regeneration. Gastroenterology 2005;128:728–741.

37. Morris JPt Cano DA, Sekine S, Wang SC, et al. Beta-catenin blocks Kras-dependent reprogramming of acini into pancreatic cancer precursor lesions in mice. J Clin Invest 2010;120:508–520.